RESEARCH ARTICLE

Proteome reference map of *Lactobacillus acidophilus* NCFM and quantitative proteomics towards understanding the prebiotic action of lactitol

Avishek Majumder[1], Abida Sultan[1], Rosa R. Jersie-Christensen[1]*, Morten Ejby[1], Bjarne Gregers Schmidt[1], Sampo J. Lahtinen[2], Susanne Jacobsen[1]** and Birte Svensson[1]*

[1] Enzyme and Protein Chemistry, Department of Systems Biology, Technical University of Denmark, Denmark
[2] Danisco Bioactives, Health & Nutrition, Kantvik, Finland

Received: March 2, 2011
Revised: May 13, 2011
Accepted: May 30, 2011

Lactobacillus acidophilus NCFM is a probiotic bacterium adapted to survive in the gastrointestinal tract and with potential health benefits to the host. Lactitol is a synthetic sugar alcohol used as a sugar replacement in low calorie foods and selectively stimulating growth of *L. acidophilus* NCFM. In the present study the whole-cell extract proteome of *L. acidophilus* NCFM grown on glucose until late exponential phase was resolved by 2-DE (pH 3–7). A total of 275 unique proteins assigned to various physiological processes were identified from 650 spots. Differential 2-DE (DIGE) (pH 4–7) of *L. acidophilus* NCFM grown on glucose and lactitol, revealed 68 spots with modified relative intensity. Thirty-two unique proteins were identified in 41 of these spots changing 1.6–12.7-fold in relative abundance by adaptation of *L. acidophilus* NCFM to growth on lactitol. These proteins included β-galactosidase small subunit, galactokinase, galactose-1-phosphate uridylyltransferase and UDP-glucose-4-epimerase, which all are potentially involved in lactitol metabolism. This first comprehensive proteome analysis of *L. acidophilus* NCFM provides insights into protein abundance changes elicited by the prebiotic lactitol.

Keywords:
2-D DIGE / *Lactobacillus acidophilus* NCFM / Lactitol / Microbiology / Prebiotics / RT-PCR

1 Introduction

Lactobacillus acidophilus NCFM (NCFM) is a well-documented probiotic [1] with a 2.0 Mb genome of low G+C content (34.7%) and encoding 1862 predicted ORFs (http://www.ncbi.nlm.nih.gov; NCBI:CP000033) [2], including several transport systems and 37 glycoside hydrolases (GH) (http://www.cazy.org/) involved in uptake and utilization of carbohydrates [1, 3]. NCFM has the capacity to adapt its metabolic machinery in response to the gut nutrient composition by negative transcriptional regulation. This metabolic flexibility ensures survival of NCFM in a low nutrient and highly competitive environment [4]. In addition, NCFM contains a suite of mucus-binding proteins as an adaptation to survive in the gastrointestinal tract (GIT) [5, 6].

Correspondence: Professor Birte Svensson, Enzyme and Protein Chemistry, Department of Systems Biology, Technical University of Denmark, Søltofts Plads, Building 224, DK-2800 Kgs. Lyngby, Denmark
E-mail: bis@bio.dtu.dk
Fax: +45-45886307

Abbreviations: CAAI, codon–anticodon adaptation index; **CCR,** carbon catabolite repression; **GH,** glycoside hydrolase; **GIT,** gastrointestinal tract; **HPr,** histidine-containing phosphocarrier protein; **LAB,** lactic acid bacteria; **LABSEM,** lactic acid bacteria semisynthetic medium; **NCFM,** North Carolina Food Microbiology; note that NCFM is used as short for *Lactobacillus acidophilus* NCFM; **PEP-PTS,** phosphoenolpyruvate-phosphotransferase system; **PTM,** post-translational modification

*These authors contributed equally to this work.

**Additional corresponding author: Associate Professor Susanne Jacobsen
E-mail: sja@bio.dtu.dk

Colour Online: See the article online to view Figs. 2, 4 and 6 in colour.

Lactitol (4-*O*-*β*-D-galactopyranosyl-D-glucitol) is a synthetic sugar alcohol obtained from lactose and used as a prebiotic. It is not metabolized by humans due to lack of a suitable *β*-galactosidase and is also not absorbed in the small intestine. Lactitol therefore becomes readily accessible to the microbiota in the colon [7] and has been shown to stimulate growth and metabolism of intestinal *Bifidobacterium* and *Lactobacillus* species, thus creating unfavorable conditions for pathogens such as *Clostridia* and *Enterobacteriaceae* [8]. Daily consumption of the synbiotic combination of NCFM and lactitol by elderly volunteers increased stool frequency, fecal levels of NCFM and genus *Bifidobacterium*, and modulated fecal immune biomarkers, reflecting stimulation of intestinal mucosal functions [9]. Complementary beneficial effects with this synbiotic were also observed in a semi-continuous colon fermentation model [10].

In the present work, a comprehensive whole-cell extract reference proteome of NCFM grown with glucose as a carbon source was established using 2-DE (pH 3–7). This signature proteome with most proteins distributed in the p*I* 4–7 range was used for understanding the protein abundance dynamics associated with stimulation by the prebiotic lactitol. Comparative proteomics using 2-D DIGE (pH 4–7) coupled with mass spectrometric protein identification, revealed proteins involved in the lactitol metabolism.

2 Materials and methods

2.1 Growth conditions and protein extraction

L. acidophilus NCFM (Danisco USA, Madison, WI, USA) was grown under aerobic conditions without agitation at 37°C in 40 mL batch cultures in semisynthetic medium for lactic acid bacteria (LABSEM) [3] supplemented with 1% of either glucose or lactitol (Danisco) for soluble whole-cell proteome (p*I* 3–7) and DIGE analyses. Cultures were sub-cultured in the LABSEM for three cycles prior to analysis to avoid chemical carry-over effects. Late-log phase cells with an A_{600} nm of 2.0 for glucose and 0.4 for lactitol (Fig. 1) were harvested from four independent cultures by centrifugation (3200 × *g*, 10 min, 4°C). Cell pellets were washed twice with 0.9% NaCl, vacuum-dried without heating for approx. 2 h until dry (SpeedVac, Savant, SC110A with Vacuum unit UVS400A; GMI, Ramsey, MN, USA) and kept at −80°C until use. Cells were disrupted by manual mechanical grinding with a small number of acid washed glass beads (<100 μm diameter) using a rounded glass Pasteur pipette.

2.2 Sample preparation for 2-DE and DIGE

The disrupted cells were heated (100°C, 2 min) after addition of 60 μL sample buffer (28 mM Tris-HCl, 22 mM Tris-base pH 8.5, 0.3% SDS, 100 mM DTT). The mixture was incubated at room temperature (5 min) followed by addition of

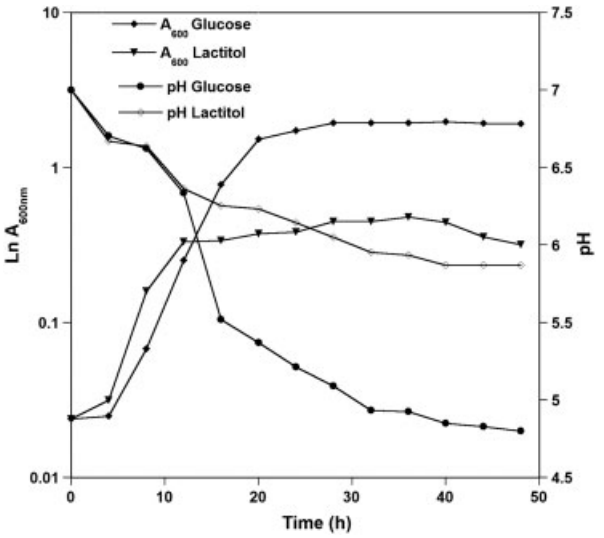

Figure 1. Growth curve and pH profile of *Lactobacillus acidophilus* NCFM grown on LABSEM with 1% of either glucose or lactitol. The late-log phase cultures, harvested at 20 h for glucose (A_{600} = 2.0) and 12 h cultures for lactitol and (A_{600} = 0.4), were used for the proteomic study.

240 μL pharmalyte buffer (8 M urea, 2 M thiourea, 100 mM DTT, 2% pharmalyte pH 4–7 (GE Healthcare, Uppsala, Sweden), 0.52% Triton X-100). The mixture was vortexed, centrifuged (10 000 × *g*, 10 min), and the supernatant was collected. Protein concentration of the supernatant was quantified (2D Quant kit; GE Healthcare) and the samples were stored at −80°C. Whole-cell extract (400 μg protein) was added to rehydration buffer (8 M urea, 2 M thiourea, 2% CHAPS, 0.5% pharmalyte 4–7, 0.3% DTT) up to 450 μL and applied on IPG strips (linear pH 3–7; 24 cm). For DIGE analysis, a dye-swapping approach was used to avoid bias due to the interference from gel fluorescence properties at different wavelengths [11]. Protein aliquots (50 μg) of each of four biological replicates grown on glucose or lactitol were labeled interchangeably with 400 pmol of either Cy3 or Cy5, vortexed, and left in the dark (30 min, 4°C). In a similar manner, aliquots (25 μg protein) of each sample were combined for internal standard and labeled with 400 pmol Cy2. Labeling reactions were quenched by 1 μL 10 mM lysine in the dark (10 min). The internal standard and the samples were mixed and the volume was made to 450 μL with rehydration buffer for IPG strips (linear pH 4–7, 24 cm).

2.3 2-DE for whole-cell extract proteome and differential proteomics

Separation in the first dimension was performed using IPG strips (pH 3–7; 24 cm; GE Healthcare) on Ettan™ IPGphor (GE Healthcare). The reference map showed few proteins of p*I* < 4, hence for DIGE pH 4–7 IPG strips were used. After rehydration at 20°C for 12 h at 50 μA/strip, IEF was

performed to a total of 78 kVh (1 h at 150 V, 1 h at 300 V, 1 h at 1000 V, gradient to 8000 V, hold at 8000 V until a total of at least 78 kVh was reached). Subsequently, strips were equilibrated (2 × 15 min) in 5 mL equilibration buffer (6 M urea, 30% glycerol, 50 mM Tris-HCl, pH 8.8, 2% SDS, 0.01% bromophenol blue) supplemented with 1% DTT and 2.5% iodoacetamide in the first and second equilibration steps, respectively. The strips and molecular weight (*Mr*) markers (Mark 12™, Invitrogen) were placed on 12.5% SDS-PAGE gels and overlaid with 0.5% molten agarose in 1 × SDS running buffer (0.25 M Tris-base, 1.92 M glycine, 1% SDS). The second dimension (SDS-PAGE) was performed on Ettan™ DALT *twelve* Electrophoresis Unit (GE Healthcare) overnight at 1 W/gel until the dye front reached the gel bottom. The proteome reference map gels (pH 3–7) were stained by colloidal CBB as described previously [12].

2.4 Image analysis

Images of colloidal CBB stained gels were generated (Microtek scanner; Scan maker 9800XL; Microtek, Carson, USA) using the Photoshop CS4 software and image analysis was done using the algorithm for blob images [13]. Imaging of DIGE gels (four biological replicates and four internal standard gels) was done immediately after the second dimension run at excitation/emission wavelengths of Cy2 (488/520 nm), Cy3 (532/580 nm) and Cy5 (633/670 nm), respectively (100 μm resolution; Typhoon 9410 Variable Mode Imager; GE Healthcare). Gel images were aligned by automated calculation of ten manually assigned alignment landmark vectors (Progenesis SameSpots version 3.3, nonlinear Dynamics, Newcastle upon Tyne, UK). Scanned gels were analyzed by intra-gel (difference in-gel) and inter-gel (biological variance) analysis. A 1.5-fold threshold (spot volume ratio change and ANOVA $p<0.05$ and a false discovery rate of $q<0.05$) was chosen as criterion in the identification of differentially expressed protein candidates. The 1.5-fold threshold value used was based on the Power analysis, which has a recommended value of 80%. Power analysis can be used to calculate the minimum sample size required to accept the outcome of a statistical test with a particular level of confidence [14]. The experimental setup had enough statistical power with the four replicate gels. False discovery rate estimates the number of false positives within statistically significant changes in the experiment [15]. The q value was set to <0.05 giving a false discovery rate of 5%. Gels were post-stained with colloidal CBB prior to spot protein identification.

2.5 In-gel digestion and protein identification by MS

Spots on 2-DE reference map and DIGE gels were excised manually and subjected to in-gel tryptic digestion with modifications as described below [16]. Gel pieces were washed with 100 μL 40% ethanol (10 min) followed by 50 μL 100% ACN, and incubated 45 min on ice with 2 μL 12.5 ng/μL trypsin (Promega) in 25 mM ammonium bicarbonate followed by addition of 10 μL 25 mM ammonium bicarbonate for rehydration, and incubated at 37°C overnight. A supernatant aliquot (1 μL) was applied to the Anchor Chip target (Bruker-Daltonics, Bremen, Germany), covered by 1 μL matrix solution (0.5 μg/μL CHCA in 90% ACN, 0.1% TFA) and washed in 0.02% TFA. MS and MS/MS spectra were obtained by Ultraflex II MALDI-TOF MS mass spectrometer (Bruker-Daltonics) in auto-mode using Flex Control v3.0 (Bruker-Daltonics) and processed by Flex Analysis v3.0 (Bruker-Daltonics). Peptide mass maps were acquired in reflectron mode with 500 laser shots per spectrum. Spectra were externally calibrated using a tryptic digest of β-lactoglobulin (5 pmol/μL); MS/MS data were acquired with stop conditions so that 1000–1600 laser shots were accumulated for each spectrum. The MS together with MS/MS spectra were searched against the NCBInr database for bacteria (NCBInr 20090826; 9 523 564 sequences; 3 256 669 569 residues) using the MASCOT 2.0 software (http://www.matrixscience.com) integrated together with BioTools v3.1 (Bruker-Daltonics). Search parameters were monoisotopic peptide mass accuracy of 80 ppm, fragment mass accuracy to ±0.7 Da; maximum of one missed cleavage; carbamidomethylation of cysteine and partial oxidation of methionine. Filtering of peaks was carried out for known keratin and autocatalytic trypsin peaks; the signal-to-noise threshold ratio was set to 1:6. Protein identifications by PMF were confirmed with a MASCOT score of 80, $p\leq0.05$ and should have a minimum of six matched peptides. Single peptide-based protein identifications by MS/MS analysis were confirmed with a MASCOT score of 40, $p\leq0.05$.

2.6 Semiquantitative RT-PCR

Total RNA from glucose and lactitol grown cultures was extracted using the Trizol (Invitrogen) method according to manufacturer's instructions. RNA was purified by Pure link RNA minikit with on-column DNase treatment to remove contaminating DNA. The primer pairs were designed using the Primer3 software (http://frodo.wi.mit.edu/primer3/) and 1 μg of total RNA was used as the template for reverse transcription of nine selected genes with Omniscript reverse transcriptase by OneStep RT-PCR (Qiagen) according to manufacturer's instructions. PCR was carried out with the primer pairs (Supporting Information Table 1) in a Thermal cycler (PTC-200 Peltier Thermal Cycler, GMI, Ramsey, US-MN) (50°C for 30 min, 95°C for 15 min, followed by 22 three-step cycles of 94°C for 1 min, 55°C for 1 min and 72°C for 1 min). NCFM 16S ribosomal DNA (rDNA) (LBA2001 and LBA2071) transcript whose expression is always constant was used as internal control [17]. The absence of

DNA contamination in the RNA preparation was confirmed according to manufacturer's instructions (Qiagen), by heat inactivation of Omniscript reverse transcriptase. The PCR products were detected by 2% agarose gel electrophoresis with ethidium bromide staining.

2.6 In silico analysis

The codon–anticodon adaptation index (CAAI) of all ORFs of NCFM was obtained using DAMBE (http://dambe.bio.uottawa.ca/dambe.asp) [18] in two steps. First, CAAI values were created using the codon table based on tRNA anticodons frequency, without a reference set of highly expressed genes. The CAAI values were then adjusted to a range of 0−1 [18]. GRAVY values were calculated using the ProtParam tool (http://www.expasy.ch/tools/protparam.html).

3 Results and discussion

3.1 Growth of NCFM on glucose and lactitol

Detailed growth curves and pH profiles of NCFM grown with glucose or lactitol as a carbohydrate source (Fig. 1) showed higher cell density and larger decrease in pH of cultures with glucose as compared with lactitol. Proteome changes with the prebiotic were determined at late exponential phase cultures under controlled conditions, because this is the stage with maximum synthesis of macromolecules [19] and where accumulation of stress proteins is minimal. The growth phase significantly affects the proteome pattern and in the stationary phase, stress-sensing and stress-related proteins are produced due to depletion of nutrients [19–21].

3.2 The reference map of the NCFM proteome (pH 3–7)

A reference map using whole-cell extract of NCFM grown on LABSEM medium was established to identify constitutively expressed proteins and to describe the dynamics of this proteome in response to carbohydrate prebiotics. Initially, the wide range of pH 3–10 (linear; 18 cm; data not shown) was used for separation in the first dimension to get an overview of the NCFM proteome distribution on the 2-DE. However, since the vast majority of spots clustered at pH 4–7, IEF in pH 3–7 was applied to optimize spot resolution in the densely populated area of the 2-D-gel. Six hundred and fifty well-resolved spots were selected for identification from the CBB stained 2-D-gel (Fig. 2), which led to 507 protein identifications using MALDI-TOF MS and/or MS/MS (Supporting Information Tables 2 and 3; Supporting Information Figs. 2 and 3). Several proteins appeared in more than one spot and in total 275 unique proteins were identified (Supporting Information Tables 2 and 3). Only 16 of the 275 unique proteins have theoretical pI > 7.0 and most of these were identified from spots shaped as horizontal streaks in the pH range 3–7 (Fig. 2). Proteins present in more than one spot showing pI and *Mr* heterogeneity were probably post-translationally modified (PTM)

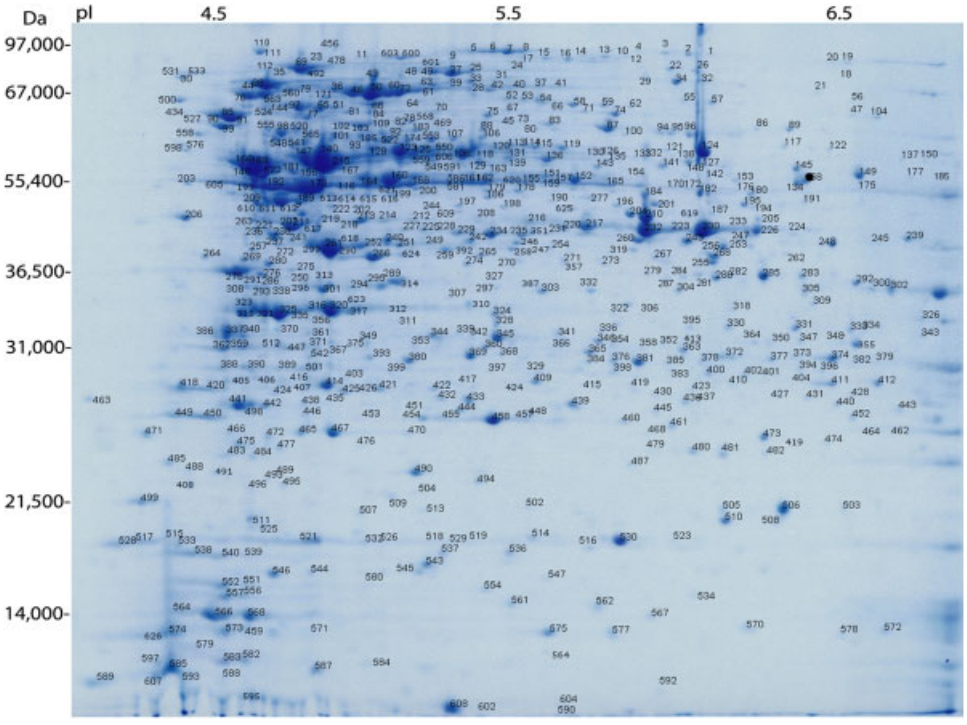

Figure 2. A detailed 2-DE of the 400 μg whole-cell extract soluble proteins (pH 3–7) of *Lactobacillus acidophilus* NCFM grown on LABSEM with 1% glucose. Numbered spots are chosen for analysis by in-gel digestion and mass spectrometry.

or found as highly similar isoforms. Isoelectric heterogeneity in 2-DE is very common in proteomics [19, 22–24] and has been attributed to PTM or to artifacts, e.g. carbamylation by urea or deamidation [22]. Carbamylation generally leads to spot charge trains, not observed on the NCFM 2-DE (Fig. 2) and the multiple protein forms probably stem from PTM. During the past years a number of proteome 2-DE profiles were described for lactic acid bacteria (LAB) [25] mostly related to studies of changes associated with growth [19, 20, 24], growth medium [26] and adaptations to the gut [27, 28]. However, very few proteome reference maps were reported [19, 29, 30]. For example, using narrow range pH windows of 4–7 and 4.5–5.5 a reference map of *Lactococcus lactis* IL14103 contained 230 proteins, corresponding to 25% coverage of the predicted acidic proteome [29]. Proteome analysis of cytosolic proteins of *L. plantarum* WCFS1 at pH range 3–10 covered 3.3% of all genes [19]. The present 275 unique proteins identified in the NCFM proteome, comprising 259 proteins of p*I* 3–7 and 16 proteins with p*I* > 7, constitute approximately 15% coverage of the theoretical proteome and 36% of the predicted intracellular acidic proteome. Proteome coverage was 3.3–21.4% in proteome studies of other Gram-positive bacteria [19, 21, 29, 31].

3.3 In silico analysis and the experimental proteome

The NCFM in silico proteome generated using the bioinformatics tool JVirGel version 2 (http://www.jvirgel.de/) contains 705 intracellular proteins of p*I* 3–7 and *Mr* 5–200 kDa. The 259 identified proteins (p*I* 3–7 range) thus constitute 36% of the theoretical proteome. Grouping the identified proteins according to functionality using Gene Role Category annotation (http://cmr.jcvi.org/tigr-scripts/CMR/CmrHomePage.cgi) (Fig. 3; Supporting Information Tables 2 and 3) showed the majority are important in protein synthesis and energy metabolism. Proteins associated with protein synthesis were dominated by components of the translational machinery, whereas proteins related to energy metabolism were dominated by enzymes of the glycolysis/gluconeogenesis. The current proteomics data complements an earlier transcriptome analysis of global gene expression patterns of NCFM grown on eight different carbohydrate sources with glycolysis genes being consistently highly expressed [4]. The cellular localization was predicted using PSORT version 3.0 (http://www.psort.org/) (Supporting Information Tables 2 and 3), which indicated that 218 of the 275 identified proteins were cytoplasmic, 10 belonged to the cytoplasmic membrane, two were extracellular, two were associated with cell wall formation and 43 had unknown cellular localization.

One of the limitations of 2-D-gel-based proteomics is poor detection of low-abundance proteins. The theoretical abundance of proteins on 2-D-gels can be calculated using the CAAI, which is based on the codon usage bias and the relative frequencies of tRNA anticodons [18]. CAAI is an indicator of translation efficiency used to predict gene expression levels in bacteria. Several recent reference proteomes used CAAI analyses to assess the genome with respect to the translation efficiency [21, 29, 31]. The relative abundance of proteins on the reference 2-D-gel (pH 3–7) correlated with the predicted CAAI values, the high- and low-abundant proteins having high and low CAAI values, respectively (Fig. 2 and Supporting Information Fig. 1A). Thus CAAI values for proteins from the most

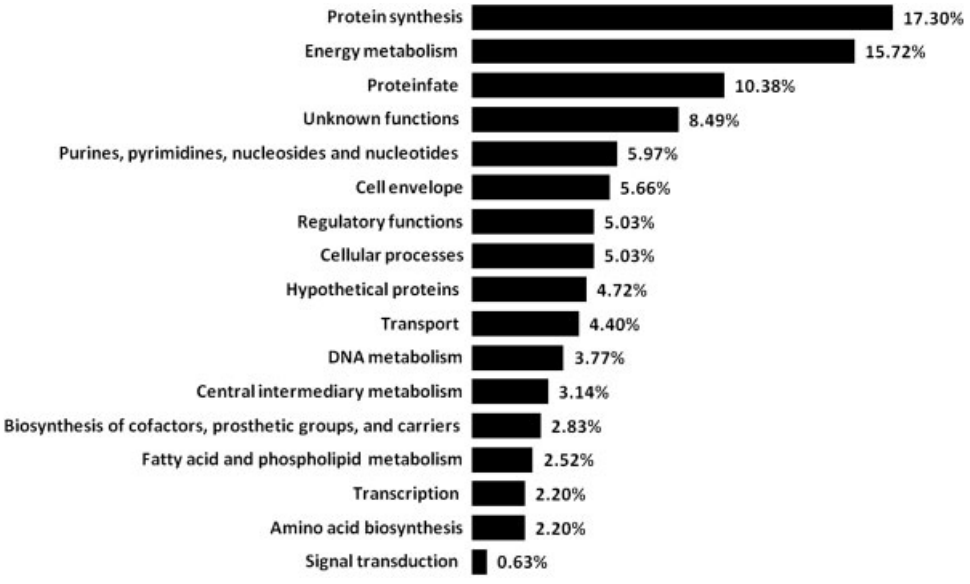

Figure 3. Functional grouping of the 275 identified unique proteins on the 2-DE (pH 3–7) of *Lactobacillus acidophilus* NCFM.

intensely stained spots, e.g. elongation factor Tu (EF-Tu) (spot 140, 147, 215), L-LDH (spot 261, 299, 290), glyceraldehyde-3-P dehydrogenase (spot 230, 232, 210), pyruvate kinase (spot 46, 50, 60) and phosphopyruvate hydratase (spot 169, 166, 140) were in the 0.581–0.69 range. Noticeably, among 23 proteins with CAAI <0.2, indicating low abundance, 10 were identified from the 2-D-gel. The GRAVY index for hydrophobicity of all NCFM coding sequences was calculated and proteins identified from the 2-D-gel have values from 0.179 to -1.244 (Supporting Information Fig. 1B). Only 18 identified proteins have a GRAVY value >0, and hydrophobic proteins with values >0.2 were not identified due to loss during sample preparation and/or electrophoresis. The present percentage of hydrophobic proteins identified on the 2-D-gel is similar to the previous reference proteomes of bacteria [21, 31].

3.4 Identification of differentially abundant proteins with NCFM grown on lactitol

Proteome changes of NCFM elicited by growth on lactitol compared with glucose (Fig. 4) were identified using 2-D DIGE. The predicted cytosolic proteome has a total of 17 proteins of p$I<4.0$, but only one, DNA-directed RNA polymerase subunit delta (LBA0232) (spot 463), was identified on the reference 2-D-gel (Supporting Information Table 2). DIGE was therefore performed at pI 4–7 to obtain better spot resolution. A total of 68 spots changed >1.5-fold in relative abundance. Forty-one identified spots representing 32 unique proteins were differentially abundant in response to lactitol (Table 1), with 25 up-regulated (1.6–12.7-fold) and 16 down-regulated (1.6–4.8-fold) proteins/protein forms (Fig. 4 and Table 1). Certain proteins, such as galactokinase (spot 628, 629), mannose-6-phosphate isomerase (spot 630), fructokinase (spot 637) and deoxyadenosine kinase (spot 634), were identified from the DIGE experiment (Fig. 4), but absent in the reference 2-D-map. The present DIGE data show that abundant enzymes apparently responsible for the utilization of lactitol are essentially identical to the metabolic machinery for utilization of lactose, i.e. the Leloir pathway. As will be further discussed below, it offers a view of how the physiology of NCFM adapts to lactitol and its hydrolysis products (galactose and glucitol/sorbitol).

3.5 Validation of differentially abundant proteins by semiquantitative RT-PCR

To confirm the differential abundance of proteins found by DIGE, semiquantitative RT-PCR was carried out for seven gene transcripts of the Leloir pathway; β-galactosidase large subunit; β-galactosidase small subunit; galactokinase; galactose-1-phosphate uridylyltransferase; lactose permease, phosphoglucomutase and fructokinase. The results showed different expression patterns with glucose and lactitol consistent with the 2-D DIGE analysis (Fig. 5A and B).

3.6 Galactose metabolism in NCFM

Lactose has to be hydrolyzed either by a phospho-β-galactosidase (LacG), generating glucose and galactose-6-P, or by a β-galactosidase (LacZ or LacLM) to glucose and galactose [32]. In this context, β-galactosidase small subunit (LacM, LBA1468) was highly abundant (12.7-fold up-regulated) on lactitol, whereas the large subunit of the heterodimeric β-galactosidase (LacLM), belonging to GH2 (CAZy; http://www.cazy.org/) was not identified on the gel. Similarly, most enzymes for galactose metabolism were identified on 2-D-gels of *L. lactis* grown on lactose, but not the β-galactosidase [29]. The other highly abundant proteins (4.5–5.0-fold up-regulated) include galactokinase, galactose-1-phosphate uridylyltransferase and UDP-glucose-4-epimerase from the Leloir pathway (Figs. 4 and 6). Galactose-1-P generated by ATP-dependent galactokinase is transferred to UDP-glucose by galactose-1-phosphate uridylyltransferase in exchange with glucose-1-P. UDP-glucose-4-epimerase converts the generated UDP-galactose into UDP-glucose, which enters the glycolysis after phosphorylation to glucose-6-P by phosphoglucomutase, which was also 1.6-fold more abundant on lactitol (Fig. 6 and Table 1).

The genes for lactose and galactose metabolism are distributed in two adjacent loci LBA1457–1459 and LBA1462–1469 in NCFM. In LAB the organization of *lac* and *gal* clusters can vary significantly, possessing or lacking operon-like structures and genes interspersed with insertion sequences [33]. The presence of lactose permease belonging to the glycoside-pentoside-hexuronide:cation symporter family, and the enzymes of the Leloir pathway suggests lactitol is transported into NCFM by lactose permease (LacS), rather than by a phosphoenolpyruvate-phosphotransferase system (PEP-PTS) system [34]. The RT-PCR analysis confirms the clear up-regulation of *lacS* in lactitol compared to glucose (Fig. 5A and B). These results complement previous extensive transcriptomic studies of NCFM grown on different carbohydrates [3, 4]. In the transcriptomic study with lactose and galactose, 10 different genes within the *lac* and *gal* loci were shown to be significantly up-regulated, *galKTME* being increased 2.7–17.6-fold, and *lacSZL* 2.8–29.5-fold [4]. The *lac-gal* locus region has two β-galactosidase genes *lacZ* (LBA1462) and *lacLM* (LBA1467-68) of the GH42 and GH2 families, respectively, and the *lacZ* gene was significantly overexpressed in the transcriptome study [4]. The two β-galactosidases, were not identified in the present 2-DE, except for the small subunit of β-galactosidase (LacM). Thus the proteome analysis did not indicate which β-galactosidase acts on lactitol, but since the large subunit of β-galactosidase (*lacL*) was found to be highly expressed by semiquantitative RT-PCR (Fig. 5A and B) we propose that LacLM catalyses the hydrolysis of lactitol.

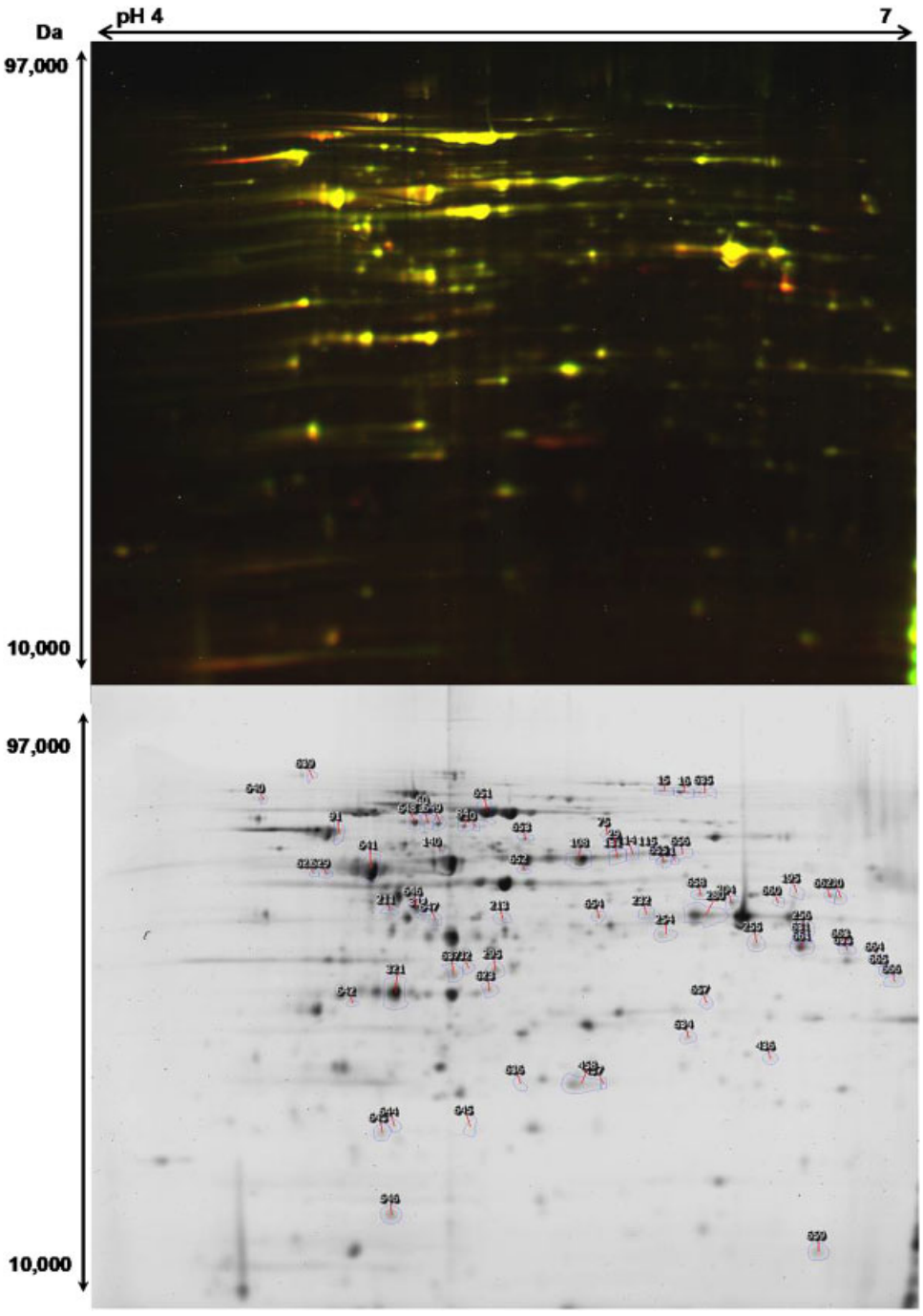

Figure 4. Representative 2-D DIGE images of whole-cell extract soluble proteins of *Lactobacillus acidophilus* NCFM grown on glucose (Cy3 green) and lactitol (Cy5 red) and the corresponding gray scale image of the CBB stained gel. The numbers on the gel indicate spots picked for identification by mass spectrometry.

3.7 Sorbitol metabolism in NCFM

The DIGE analysis showed various enzymes involved in glucitol/sorbitol metabolism to be more abundant (1.7–4.3-fold; Table 1 and Fig. 6) in the presence of lactitol. Sorbitol in NCFM is metabolized to fructose-6-P, ultimately leading to either glycolysis or fructose and mannose metabolism according to the KEGG pathway (Kyoto Encyclopedia of Genes and Genomes; http://www.genome.ad.jp/kegg) [35]. Sorbitol has been described as a carbon source for certain Gram-positive bacteria, including LAB and enzymes for sorbitol metabolism are encoded by an operon-like structure and subject to catabolite repression by glucose in Gram-positive bacteria [36, 37]. This kind of organization for sorbitol utilization was not identified in the NCFM genome. The phosphotransferase system enzyme II (PTS EII, LBA0655) based on its conserved domains belongs to the class of PEP-PTS specific for glucitol (http://pfam.sanger.ac.uk/) [38]. The PTS components are involved in the phosphorylation of carbohydrate by the histidine-containing

Table 1. Protein identifications of differentially abundant spots ($\geq$1.5-fold spot volume ratio change and ANOVA $p \leq 0.05$) of *Lactobacillus acidophilus* NCFM grown on SEM medium with 1% glucose and 1% lactitol

Spot	Accession number	Protein description	Score	Sequence coverage %	Peptides matched/ searched	MW/p*I*	Fold change
254	gil58337734	β-Galactosidase small subunit	124	38	10/45	35 966/5.53	+12.7
628	gil58337726	Galactokinase	100	37	12/56	43 521/4.74	+5.0
29	gil58337725	Galactose-1-phosphate uridylyltransferase	146	43	20/68	55 735/5.48	+4.8
311	gil58336405	D-Lactate dehydrogenase	135	38	13/34	39 177/4.96	−4.8
255	gil58337735	UDP-glucose 4-epimerase	163	37	14/36	36 458/5.95	+4.7
457	gil58336994	Phosphate starvation inducible protein stress related	113	48	12/71	21 503/5.46	+4.4
630	gil58337059	Mannose-6-phosphate isomerase	98	37	11/48	36 677/6.03	+4.3
458	gil58336994	Phosphate starvation inducible protein stress related	130	63	15/77	21 503/5.46	+4.2
631	Mixture						+3.9
	gil58337735	UDP-glucose 4-epimerase	235	76	25/92	36 458/5.95	
	gil58336950	UTP-glucose-1-phosphate uridylyltransferase	118	57	15/92	33 875/5.90	
632	gil58337322	Oxidoreductase	124	42	13/63	31 816/5.19	+3.9
211	gil58336405	D-Lactate dehydrogenase	141	50	18/67	39 177/4.96	+3.3
633	gil58337735	UDP-glucose 4-epimerase	303	83	30/85	36 458/5.95	+3.1
623	gil58337488	Hypothetical protein LBA1206	170	42	12/42	31 352/5.15	+3.1
16	gil58336392	Ribonucleoside triphosphate reductase	289	46	33/73	83 982/5.62	+2.9
634	gil58338190	Deoxyadenosine kinase	79	30	7/44	24 765/5.70	−2.9
635	gil58336733	Putative oxalyl-CoA decarboxylase	228	42	25/71	60 969/5.03	−2.9
213	gil58337704	Dihydroxyacetone kinase	110	36	12/44	36 307/5.16	+2.8
636	gil58336994	Phosphate starvation inducible protein stress related	79	33	7/24	21 503/5.46	+2.8
436	gil58337318	Oxidoreductase	104	49	9/23	23 070/5.78	+2.6
140	gil58337152	Elongation factor Tu	176	50	19/68	43 609/4.97	+2.6
637	gil58336369	Fructokinase	161	50	17/45	32 016/5.08	+2.4
232	gil58337019	Glyceraldehyde-3-P dehydrogenase	138	37	12/35	36 643/5.92	+2.3
321	gil58337860	Fructose-bisphosphate aldolase	206	65	21/85	33 560/4.94	−2.2
114	gil58336560	UDP-*N*-acetylglucosamine pyrophosphorylase	100	30	13/46	50 162/5.57	−2.2
195	gil58336608	Ala racemase	81	29	10/39	41 801/6.02	+2.1
295	gil58337322	Oxidoreductase	116	44	12/50	31 816/5.19	+2.1
50	gil58337255	Pyruvate kinase	233	38	29/79	63 136/5.23	+1.9
15	gil58336392	Ribonucleoside triphosphate reductase	91	13	10/26	83 982/5.62	−1.9
638	gil58336743	Chaperonin GroEL	167	45	15/97	57 785/4.98	−1.9
280	gil58337019	Glyceraldehyde-3-P dehydrogenase	239	76	24/97	36 643/5.92	+1.8
256	gil58337089	F_0F_1 ATP synthase subunit γ	136	42	18/73	35 512/5.93	−1.8
130	gil58336600	Serine hydroxymethyl transferase	112	26	12/44	45 276/5.56	−1.8
91	gil58337153	Trigger factor	93	34	17/90	49 275/4.72	−1.7
546	gil58336978	Phosphotransferase system enzyme II	105	55	9/38	13 904/4.84	+1.7
84	gil58337008	Phosphoglucomutase	186	47	26/100	64 122/5.18	+1.6
204	gil58336540	Inosine-5′-monophosphate dehydrogenase	247	63	24/96	39 816/5.75	−1.6
115	gil58336750	Glucose-6-P 1-dehydrogenase	157	39	17/43	55 824/5.57	−1.6
75	gil58337220	Citrate lyase α chain	116	29	13/36	55 315/5.53	−1.6
108	gil58338136	Adenylosuccinate synthetase	157	51	21/82	47 851/5.38	−1.6
131	gil58338136	Adenylosuccinate synthetase	185	55	23/95	47 851/5.38	−1.6

Protein identifications were confirmed with a MASCOT score of 80 for peptide mass fingerprint and ANOVA $p \leqslant 0.05$, and a minimum of six matched peptides.

phosphocarrier protein (HPr). HPr is in turn phosphorylated by the PEP system or by ATP-dependent auto-phosphorylation [39]. PTS EII (LBA0655), phosphorylating glucitol to glucitol-6-phosphate, was 1.7-fold more abundant (Fig. 6), and the two oxidoreductases (LBA1023 and LBA1027) were 2.9- and 3.9-fold more abundant in lactitol, respectively. These oxidoreductases (LBA1023 and LBA1027) may be involved in the interconversion of

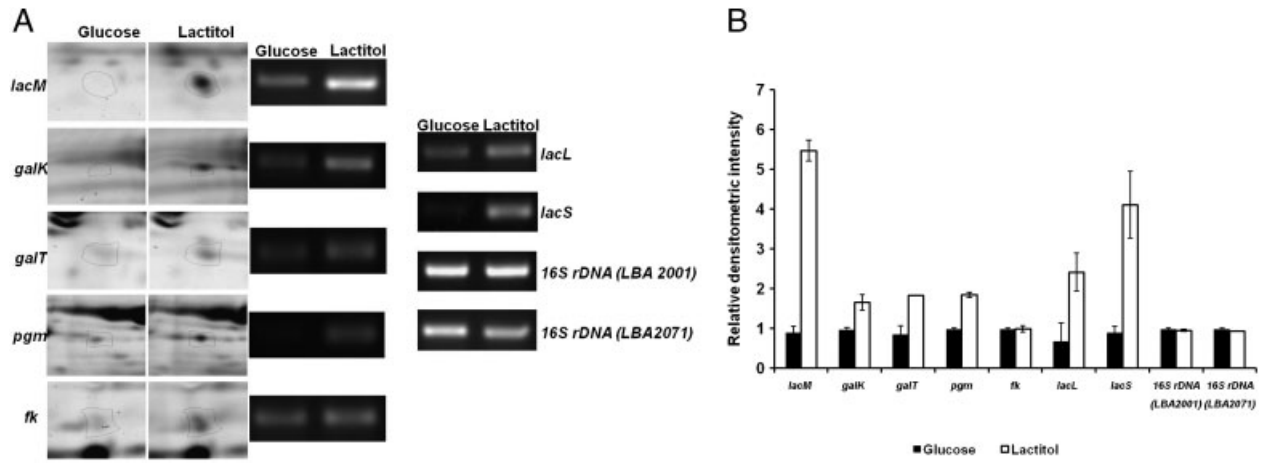

Figure 5. (A) The semiquantitative RT-PCR amplified fragments of selected genes of *Lactobacillus acidophilus* NCFM grown on SEM medium with 1% glucose and 1% lactitol. The expression of 16S rDNA was used as an internal control. *lacM*, β-galactosidase small subunit; *galK*, galactose kinase; *galT*, galactose-1-phosphate uridylyltransferase; *pgm*, phosphoglucomutase; *fk*, fructokinase; *lacL*, β-galactosidase large subunit; *lacS*, lactose permease. (B) Bar graphs showing density measurements of bands after background level subtraction of the selected genes of *Lactobacillus acidophilus* NCFM grown on SEM medium with 1% glucose and 1% lactitol. The values are expressed compared to density measurement of glucose which is fixed arbitrarily at 1. The data presented are averages of two independent experiments, and error bars represent standard deviations.

D-glucitol-6-P to L-sorbose-1-P and maintain the concentrations of glucitol-6-P (KEGG). Glucitol-6-P has to be converted to β-D-fructose-6-P by 6-phosphogluconate dehydrogenase, which was not identified by DIGE (Fig. 6). β-D-Fructose-6-P is the central metabolite that can either enter glycolysis, amino sugar metabolism, or be converted to other carbohydrate metabolites. The other significantly differentially abundant enzymes were mannose-6-phosphate isomerase and fructokinase, which increased by 4.3- and 2.4-fold, respectively. The β-D-fructose-6-P generated by sorbitol catabolism may thus enter either fructose or mannose metabolism or it enters glycolysis after being converted to β-D-fructose-1,6-bis-P by phosphofructokinase. Fructose-bisphosphate aldolase decreased (2.2-fold) and there was an increase of glyceraldehyde-3-P dehydrogenase (2.3-fold) and dihydroxyacetone kinase (2.8-fold) (Table 1), which might channel all β-D-fructose-1,6-bis-P into glycolysis.

3.8 Carbon catabolite repression (CCR) and the enzymes of glycolysis

In low G+C Gram-positive bacteria, PTS protein and HPr are the master regulators of carbon flow and metabolism. The phosphorylation and dephosphorylation of these proteins control the carbon metabolism via CCR [39, 40]. The CCR regulatory network in NCFM was also observed by microarray data with the presence of a flexible transcriptome controlled by CCR [4]. The key gene products involved in the regulation, i.e. catabolite control protein A (CcpA), HPr, HPrK/P and PTS, were consistently highly abundant in the NCFM transcriptome, which suggested the regulation to occur at the protein rather than the transcriptional level [4]. PTS phosphotransferase activity and the phosphoenolpyruvate-to-pyruvate ratio regulates the concentrations of metabolites such as fructose-1,6-bis-P, ATP, PP_i and P_i, which in turn control the HPr kinase activity [39, 41, 42]. Various enzymes indicating the regulation in the presence of lactitol were identified by DIGE analysis. In *Streptococcus* sp. transport of lactose via lactose permease containing the IIA domain was found to be regulated at the protein level by different HPr forms [43]. A similar mechanism is possible in NCFM owing to the absence of other transporters for lactose and the presence of a highly homologous lactose permease with IIA domain. The cellular concentration of pyruvate kinase, which has control over the phosphoenolpyruvate-to-pyruvate ratio, was 1.9-fold more abundant, which indicates CCR. Lactate dehydrogenase converts the generated pyruvate into lactate and noticeably, of two different NCFM lactate dehydrogenase forms, one increased by 3.3-fold and the other decreased by 4.8-fold (Table 1).

In Gram-positive bacteria when readily metabolized carbohydrate is available as energy source, the intracellular concentration of fructose-1,6-bis-P increases and the concentrations of ATP and P_i decrease, while the opposite is true for unfavorable carbohydrate sources [39]. The presence of increased abundant enzymes for the intermediary metabolite β-D-fructose-6-P to fructose and mannose metabolism, glyceraldehyde-3-P dehydrogenase (2.3-fold), dihydroxyacetone kinase (2.8-fold) and a decrease in abundance of fructose-bisphosphate aldolase (2.2-fold) indicates β-D-fructose-6-P being converted to fructose, mannose or glyceraldehyde-3-P. This might lead to lowered concentrations of fructose-1,6-bis-P, and therefore a complete switch in the metabolic machinery [34, 39].

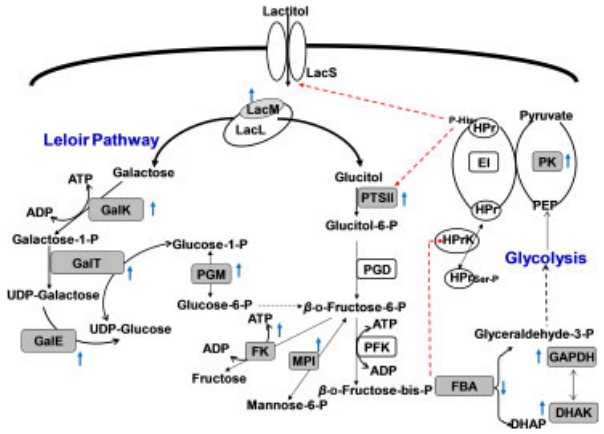

Figure 6. Schematic representation of the proposed proteins involved in lactitol metabolism. The proteins shaded in gray were identified by 2-D DIGE and MS, whereas the proteins in white were hypothesized to be involved in the metabolism of lactitol. Blue arrows by their orientation show differentially abundant proteins. Dashed red arrow shows proteins and metabolites involved in CCR. LacS, lactose permease; LacL, β-galactosidase large subunit; LacM, β-galactosidase small subunit; GalK, galactose kinase; GalT, galactose-1-phosphate uridylyltransferase; GalE, UDP-glucose-4-epimerase; PGM, phosphoglucomutase; FK, fructokinase; MPI, mannose-6-p-isomerase; PTSII, phosphotransferase component specific for glucitol; PGD, 6-phosphogluconate dehydrogenase; PFK, phosphofructokinase; FBA; fructose-bisphosphate aldolase; GAPDH; glyceraldehyde-3-p dehydrogenase; DHAK; dihydroxyacetone kinase; PK; pyruvate kinase; EI; enzyme I; HPr; histidine-containing phosphocarrier protein; HPrK/P; HPr kinase/phosphorylase. Black dashed arrow indicates the entry of glyceraldehyde-3-P into glycolysis.

More recently, glycolytic enzymes from low G+C bacteria have been ascribed multiple roles such as mucus adhesion [28], mRNA processing [44] and interactions with key regulatory proteins. These proteins are often overlooked as housekeeping genes in proteome studies, but changes in their abundance may have significant effects on the metabolic pathways. Glucose-6-phosphate 1-dehydrogenase, which is very important in maintaining the redox potential of the cell by generating NADPH, was found to be 1.6-fold lower in abundance, and phosphoglucomutase, which maintains a balance between the glucose-6-P and glucose-1-P, was found to be more abundant by 1.6-fold. Glucose-6-P is the metabolite that enters the glycolysis, and lower abundance of glucose-6-phosphate 1-dehydrogenase and higher abundance of phosphoglucomutase may lead to accumulation of glucose-1-P.

3.9 Variation of abundance in other proteins elicited by lactitol

The other differentially abundant proteins include elongation factor Tu (EF-Tu) and putative stress-related phosphate starvation inducible protein both involved in protein synthesis (http://cmr.jcvi.org/tigr-scripts/CMR/CmrHomePage.cgi). Along with its function in protein translation, EF-Tu has been reported to have a role in other cellular processes, including acting as chaperone in protein folding in *E. coli* [45]. In several LAB, EF-Tu was localized to the cell wall and described as a 'moonlighting protein', i.e. a protein that has multiple, apparently unrelated functions in different cell locations [46]. EF-Tu was moreover suggested to participate in intestinal cell adhesion [28, 46–48] and its 2.6-fold increase may be connected to the higher number of NCFM in the GIT during lactitol administration [9]. The proposed involvement of EF-Tu in intestinal adhesion of bacteria agrees with its increased abundance by lactitol. This effect presents a novel putative mechanism for synbiotic interactions between probiotics and specific prebiotics.

At harvest pH of glucose and lactitol cultures was 5.2 and 6.3 (Fig. 1), respectively, and the difference is due to higher growth rates in glucose and increased production of lactic acid. F_0F_1 ATP synthase subunit γ was 1.8-fold higher in glucose compared to the lactitol grown cultures (Table 1), which reflect its role in maintaining the proton motive force at lower pH [49]. Also, the 1.9-fold increase in chaperonin GroEL in NCFM grown on glucose may be attributed to the low pH (Table 1). Chaperonin GroEL was reported to be induced as acid stress response in *L. acidophilus* [49], *L. lactis* and *Enterococcus faecalis*, which are all LAB [25].

Several NCFM proteins lowered in abundance in the presence of lactitol, including ribonucleoside triphosphate reductase, deoxyadenosine kinase, inosine-5′-monophosphate dehydrogenase, adenylosuccinate synthase, trigger factor and citrate lyase α-chain, most of which are involved in nucleotide metabolism. *L. lactis* grown on lactose showed a similar down-regulation of pyrimidine-regulated enzymes [29]. The catabolism of galactose-1-P to glucose-1-P, a process involving UDP-glucose and UDP-galactose and the enzymes UDP-glucose-4-epimerase and galactose-1-phosphate uridylyltransferase, has been suggested to participate in the lower abundance of pyrimidine enzymes [29], and a similar physiological response may occur with lactitol.

4 Concluding remarks

The present whole-cell extract soluble reference proteome (pH 3–7) for *L. acidophilus* NCFM is the most comprehensive analysis for a probiotic bacterium to date. A dynamic view of the proteome at the late exponential phase of NCFM grown on lactitol as a sole carbon source provides insights into probiotic–prebiotic interactions, which are essential for understanding how a prebiotic source can benefit a probiotic strain and lead to selective stimulation of its growth. *L. acidophilus* NCFM has the capacity to metabolize the carbohydrate moieties generated from lactitol. Galactose thus likely enters the Leloir pathway, while glucitol/sorbitol

is metabolized by a PTS-II component. Other proteins showing differential abundance in lactitol were indirectly involved in the CCR. Finally, lactitol increases EF-Tu that can participate in GIT adhesion processes, which presumably constitute an important consequence of intake of the synbiotic combination of NCFM and lactitol.

Birgit Andersen is acknowledged for technical assistance with mass spectrometric analysis. Dr. Rodolphe Barrangou is thanked for helpful comments to the manuscript. This work was supported by the Danish Strategic Research Council's Programme Committee on Health, Food and Welfare (FøSu), the Danish Research Council for Natural Science and the Danish Center for Advanced Food Studies (LMC). A.M. is grateful to the Technical University of Denmark for a Hans Christian Ørsted postdoctoral fellowship. A.S. thanks Danisco for a student scholarship.

The authors have declared no conflict of interest.

5 References

[1] Sanders, M. E., Klaenhammer, T. R., The scientific basis of *Lactobacillus acidophilus* NCFM functionality as a probiotic. *J. Dairy Sci.* 2001, *84*, 319–331.

[2] Altermann, E., Russell, W. M., Azcarate-Peril, M. A., Barrangou, R. et al., Complete genome sequence of the probiotic lactic acid bacterium *Lactobacillus acidophilus* NCFM. *Proc. Natl. Acad. Sci. USA* 2005, *102*, 3906–3912.

[3] Barrangou, R., Altermann, E., Hutkins, R., Cano, R., Klaenhammer, T. R., Functional and comparative genomic analyses of an operon involved in fructooligosaccharide utilization by *Lactobacillus acidophilus*. *Proc. Natl. Acad. Sci. USA* 2003, *100*, 8957–8962.

[4] Barrangou, R., Azcarate-Peril, M. A., Duong, T., Conners, S. B. et al., Global analysis of carbohydrate utilization by *Lactobacillus acidophilus* using cDNA microarrays. *Proc. Natl. Acad. Sci. USA* 2006, *103*, 3816–3821.

[5] Buck, B. L., Altermann, E., Svingerud, T., Klaenhammer, T. R., Functional analysis of putative adhesion factors in *Lactobacillus acidophilus* NCFM. *Appl. Environ. Microbiol.* 2005, *71*, 8344–8351.

[6] Ventura, M., O'Flaherty, S., Claesson, M. J., Turroni, F. et al., Genome-scale analyses of health-promoting bacteria: probiogenomics. *Nat. Rev. Microbiol.* 2009, *7*, 61–71.

[7] Grimble, G. K., Patil, D. H., Silk, D. B. A., Assimilation of lactitol, an unabsorbed disaccharide in the normal human-colon. *Gut* 1988, *29*, 1666–1671.

[8] Finney, M., Smullen, J., Foster, H. A., Brokx, S., Storey, D. M., Effects of low doses of lactitol on faecal microflora, pH, short chain fatty acids and gastrointestinal symptomology. *Eur. J. Nutr.* 2007, *46*, 307–314.

[9] Ouwehand, A. C., Tiihonen, K., Saarinen, M., Putaala, H., Rautonen, N., Influence of a combination of *Lactobacillus acidophilus* NCFM and lactitol on healthy elderly: intestinal and immune parameters. *Br. J. Nutr.* 2009, *101*, 367–375.

[10] Makivuokko, H., Forssten, S., Saarinen, M., Ouwehand, A., Rautonen, N., Synbiotic effects of lactitol and *Lactobacillus acidophilus* NCFM™ in a semi-continuous colon fermentation model. *Benef. Microbes* 2010, *1*, 131–137.

[11] Tannu, N. S., Hemby, S. E., Two-dimensional fluorescence difference gel electrophoresis for comparative proteomics profiling. *Nat. Protoc.* 2006, *1*, 1732–1742.

[12] Candiano, G., Bruschi, M., Musante, L., Santucci, L. et al., Blue silver: a very sensitive colloidal Coomassie G-250 staining for proteome analysis. *Electrophoresis* 2004, *25*, 1327–1333.

[13] dos Anjos, A., Møller, A. L. B., Ersbøll, B. K., Finnie, C., Shahbazkia, H. R., New approach for segmentation and quantification of two-dimensional gel electrophoresis images. *Bioinformatics* 2010, *27*, 368–375.

[14] Karp, N. A., Lilley, K. S., Maximising sensitivity for detecting changes in protein expression: experimental design using minimal CyDyes. *Proteomics* 2005, *5*, 3105–3115.

[15] Karp, N. A., McCormick, P. S., Russell, M. R., Lilley, K. S., Experimental and statistical considerations to avoid false conclusions in proteomics studies using differential in-gel electrophoresis. *Mol. Cell. Proteomics* 2007, *6*, 1354–1364.

[16] Hellman, U., Wernstedt, C., Gonez, J., Heldin, C. H., Improvement of an in-gel digestion procedure for the micropreparation of internal protein-fragments for amino-acid sequencing. *Anal. Biochem.* 1995, *224*, 451–455.

[17] Goh, Y. J., Zhang, C., Benson, A. K., Schlegel, V. et al., Identification of a putative operon involved in fructooligosaccharide utilization by *Lactobacillus paracasei*. *Appl. Environ. Microbiol.* 2006, *72*, 7518–7530.

[18] Xia, X. H., An improved implementation of codon adaptation index. *Evol. Bioinform. Online* 2007, *3*, 53–58.

[19] Cohen, D. P. A., Renes, J., Bouwman, F. G., Zoetendal, E. G. et al., Proteomic analysis of log to stationary growth phase *Lactobacillus plantarum* cells and a 2-DE database. *Proteomics* 2006, *6*, 6485–6493.

[20] Koistinen, K. M., Plumed-Ferrer, C., Lehesranta, S. J., Karenlampi, S. O., von Wright, A., Comparison of growth-phase-dependent cytosolic proteomes of two *Lactobacillus plantarum* strains used in food and feed fermentations. *FEMS Microbiol. Lett.* 2007, *273*, 12–21.

[21] Wu, R., Wang, W. W., Yu, D. L., Zhang, W. Y. et al., Proteomics analysis of *Lactobacillus casei* zhang, a new probiotic bacterium isolated from traditional home-made koumiss in Inner Mongolia of China. *Mol. Cell. Proteomics* 2009, *8*, 2321–2338.

[22] Len, A. C. L., Harty, D. W. S., Jacques, N. A., Stress-responsive proteins are upregulated in *Streptococcus mutans* during acid tolerance. *Microbiology – SGM* 2004, *150*, 1339–1351.

[23] Pessione, E., Mazzoli, R., Giuffrida, M. G., Lamberti, C. et al., A proteomic approach to studying biogenic amine producing lactic acid bacteria. *Proteomics* 2005, *5*, 687–698.

[24] Palmfeldt, J., Levander, F., Hahn-Hagerdal, B., James, P., Acidic proteome of growing and resting *Lactococcus lactis* metabolizing maltose. *Proteomics* 2004, *4*, 3881–3898.

[25] Champomier-Verges, M. C., Maguin, E., Mistou, M. Y., Anglade, P., Chich, J. F., Lactic acid bacteria and proteomics: Current knowledge and perspectives. *J. Chromatogr. B – Analyt. Technol. Biomed. Life Sci.* 2002, *771*, 329–342.

[26] Koskenniemi, K., Koponen, J., Kankainen, M., Savijoki, K. et al., Proteome analysis of *Lactobacillus rhamnosus* GG using 2-D DIGE and mass spectrometry shows differential protein production in laboratory and industrial-type growth media. *J. Proteome Res.* 2009, *8*, 4993–5007.

[27] Roy, K., Meyrand, M., Corthier, G., Monnet, V., Mistou, M. Y., Proteomic investigation of the adaptation of *Lactococcus lactis* to the mouse digestive tract. *Proteomics* 2008, *8*, 1661–1676.

[28] Izquierdo, E., Horvatovich, P., Marchioni, E., Aoude-Werner, D. et al., 2-DE and MS analysis of key proteins in the adhesion of *Lactobacillus plantarum*, a first step toward early selection of probiotics based on bacterial biomarkers. *Electrophoresis* 2009, *30*, 949–956.

[29] Guillot, A., Gitton, C., Anglade, P., Mistou, M. Y., Proteomic analysis of *Lactococcus lactis*, a lactic acid bacterium. *Proteomics* 2003, *3*, 337–354.

[30] Gitton, C., Meyrand, M., Wang, J. H., Caron, C. et al., Proteomic signature of *Lactococcus lactis* NCDO763 cultivated in milk. *Appl. Environ. Microbiol.* 2005, *71*, 7152–7163.

[31] Yuan, J., Zhu, L., Liu, X. K., Zhang, Y. et al., A proteome reference map and proteomic analysis of *Bifidobacterium longum* NCC2705. *Mol. Cell. Proteomics* 2006, *5*, 1105–1118.

[32] Tsai, Y. K., Lin, T. H., Sequence, organization, transcription and regulation of lactose and galactose operons in *Lactobacillus rhamnosus* TCELL-1. *J. Appl. Microbiol.* 2006, *100*, 446–459.

[33] Fortina, M. G., Ricci, G., Mora, D., Guglielmetti, S., Manachini, P. L., Unusual organization for lactose and galactose gene clusters in *Lactobacillus helveticus*. *Appl. Environ. Microbiol.* 2003, *69*, 3238–3243.

[34] Devos, W. M., Vaughan, E. E., Genetics of lactose utilization in lactic-acid bacteria. *FEMS Microbiol. Rev.* 1994, *15*, 217–237.

[35] Kanehisa, M., Araki, M., Goto, S., Hattori, M. et al., KEGG for linking genomes to life and the environment. *Nucleic Acids Res.* 2008, *36*, D480–D484.

[36] Yebra, M. J., Perez-Martinez, G., Cross-talk between the L-sorbose and D-sorbitol (D-glucitol) metabolic pathways in *Lactobacillus casei*. *Microbiology-Sgm* 2002, *148*, 2351–2359.

[37] Alcantara, C., Sarmiento-Rubiano, L. A., Monedero, V., Deutscher, J. et al., Regulation of *Lactobacillus casei* sorbitol utilization genes requires DNA-binding transcriptional activator GutR and the conserved protein GutM. *Appl. Environ. Microbiol.* 2008, *74*, 5731–5740.

[38] Finn, R. D., Tate, J., Mistry, J., Coggill, P. C. et al., The Pfam protein families database. *Nucleic Acids Res.* 2008, *36*, D281–D288.

[39] Deutscher, J., Francke, C., Postma, P. W., How phosphotransferase system-related protein phosphorylation regulates carbohydrate metabolism in bacteria. *Microbiol. Mol. Biol. Rev.* 2006, *70*, 939–1031.

[40] Monedero, V., Maze, A., Boel, G., Zuniga, M. et al., The phosphotransferase system of *Lactobacillus casei*: Regulation of carbon metabolism and connection to cold shock response. *J. Mol. Microbiol. Biotechnol.* 2007, *12*, 20–32.

[41] Kotrba, P., Inui, M., Yukawa, H., Bacterial phosphotransferase system (PTS) in carbohydrate uptake and control of carbon metabolism. *J. Biosci. Bioeng.* 2001, *92*, 502–517.

[42] Dossonnet, V., Monedero, V., Zagorec, M., Galinier, A. et al., Phosphorylation of HPr by the bifunctional HPr kinase/P-ser-HPr phosphatase from *Lactobacillus casei* controls catabolite repression and inducer exclusion but not inducer expulsion. *J. Bacteriol.* 2000, *182*, 2582–2590.

[43] Hols, P., Hancy, F., Fontaine, L., Grossiord, B. et al., New insights in the molecular biology and physiology of *Streptococcus thermophilus* revealed by comparative genomics. *FEMS Microbiol. Rev.* 2005, *29*, 435–463.

[44] Commichau, F. M., Rothe, F. M., Herzberg, C., Wagner, E. et al., Novel activities of glycolytic enzymes in *Bacillus subtilis*. *Mol. Cell. Proteomics* 2009, *8*, 1350–1360.

[45] Caldas, T. D., El Yaagoubi, A., Richarme, G., Chaperone properties of bacterial elongation factor EF-Tu. *J. Biol. Chem.* 1998, *273*, 11478–11482.

[46] Siciliano, R. A., Cacace, G., Mazzeo, M. F., Morelli, L. et al., Proteomic investigation of the aggregation phenomenon in *Lactobacillus crispatus*. *BBA – Proteins Proteom.* 2008, *1784*, 335–342.

[47] Granato, D., Bergonzelli, G. E., Pridmore, R. D., Marvin, L. et al., Cell surface-associated elongation factor Tu mediates the attachment of *Lactobacillus johnsonii* NCC533 (La1) to human intestinal cells and mucins. *Infect. Immun.* 2004, *72*, 2160–2169.

[48] Kelly, P., Maguire, P. B., Bennett, M., Fitzgerald, D. J. et al., Correlation of probiotic *Lactobacillus salivarius* growth phase with its cell wall-associated proteome. *FEMS Microbiol. Lett.* 2005, *252*, 153–159.

[49] Lorca, G. L., de Valdez, G. F., Ljungh, A., Characterization of the protein-synthesis dependent adaptive acid tolerance response in *Lactobacillus acidophilus*. *J. Mol. Microbiol. Biotechnol.* 2002, *4*, 525–532.

